Chapter 2:

Isotopes, Microbes, and Turbidity: A Multi-Tracer Approach to Understanding Recharge Dynamics and Groundwater Contamination in a Basaltic Island Aquifer

Abstract

Wells designated as groundwater under the direct influence (GUDI) of surface water have caused an ongoing boil-water advisory afflicting the island of Tutuila, American Samoa for almost a decade. Regulatory testing at these wells found turbidity and indicator bacteria spikes correlated with heavy rainfall events. However, the mechanism of this contamination has, until now, remained unknown. Surface water may reach wells through improperly sealed well casings, or through the aquifer matrix itself. In this study, three independent surface water tracers, turbidity, indicator bacteria, and water isotopes were used to assess recharge timing and determine contamination mechanisms. Results from each method were reasonably consistent, revealing average GUDI well breakthrough times of 37 ± 21 h for turbidity, 18 to 63 h for bacteria, and 1 to 5 days for water isotopes. These times match well with estimated subsurface flow rates through highly permeable aquifer materials. In contrast, where one well casing was found to be compromised, turbidity breakthrough was observed at 3 to 4 h. These results support local management decisions and show repairing or replacing wells will likely result in continued GUDI contamination. Additionally, differences in observed rainfall response for each tracer provide insight into the recharge dynamics and subsurface flow characteristics of this and other highly conductive young-basaltic aquifers.

As published in: Shuler, C. K., Dulai, H., DeWees, R., Kirs, M., Glenn, C. R., & El-Kadi, A. I. Isotopes, Microbes, and Turbidity: A Multi-Tracer Approach to Understanding Recharge Dynamics and Groundwater Contamination in a Basaltic Island Aquifer. *Groundwater Monitoring & Remediation*.

2.1 Introduction

Both groundwater and surface water resources are essential for providing drinking water to the world's increasing population. While groundwater makes up only 26% of global water use (FAO 2016), in many areas, use of groundwater offers advantages over surface water. Requirements for treating groundwater to a potable standard are often less stringent because aquifers typically provide natural filtration of particulates and generally long subsurface transit times that eventually inactivate surface-living pathogens. In the United States (U.S.), the U.S. Environmental Protection Agency (US-EPA) Surface Water Rule mandates municipal water from surface water sources be treated to remove or inactivate 99.9% (3-log) of protozoa, bacteria, and 99.99% (4-log) of viruses (US-EPA 1998). To achieve this level, filtration is typically necessary as high particulate loads can reduce the efficacy of chemical treatments. Likewise, the US-EPA Groundwater Rule mandates groundwater treatment to the same standard as surface water in sources where turbidity levels exceed 1 nephelometric turbidity unit (NTU) or microbial indicator bacteria, such as total coliforms (TC) and *Escherichia coli (E. coli),* are found. In these cases, the offending well is classified as groundwater under the direct influence of surface water (GUDI) (US-EPA 2006).

In the U.S. Territory of American Samoa, the main island of Tutuila is almost entirely reliant on groundwater. Forty-five municipal wells across the island provide at least 90% of the drinking water used by the island's ≈60,000 residents (AS-DOC 2013). To determine GUDI status of Tutuila's wells, the island's water utility, American Samoa Power Authority (ASPA), performed a GUDI test at each well in the municipal system by assessing correlation between turbidity, indicator bacteria, and rainfall. Eight of Tutuila's highest producing wells located on the Tafuna-Leone Plain were found to be GUDI wells (e.g. Vold et al. 2013). Increasing the level of treatment for water produced by these wells has proven to be cost prohibitive, therefore in 2009 a boil-water advisory was issued over much of the island. As of this writing, the boil-water advisory remains in effect for large portions of the water delivery system.

Although surface water clearly reaches some of Tutuila's wells during heavy-rainfall, the mechanism of this contamination has yet to be identified. Two hypothesized mechanisms are (1) highly-permeable aquifer material that allows surface water to infiltrate and contaminate the entire aquifer, or (2) improperly constructed well casings or well packings that allow small amounts of localized surface water to infiltrate through the well bore itself (Fig. 2.1). If contamination primarily travels through faulty well seals, then repairing or replacing the wells would be cost effective and allow continued use of existing water delivery infrastructure. However, if the permeability of the entire aquifer is so high as to lack sufficient filtration capacity, abandonment of the entire well field or installation of costly surface water treatment facilities will be necessary to solve the issue. Therefore, developing a better understanding of the recharge dynamics in the Tafuna and Leone aquifers will benefit future groundwater management efforts on Tutuila.

In this study, the aforementioned hypotheses were tested by comparing levels of environmental tracers with rainfall records to determine the average travel time of surface water to each GUDI well. Three independent multi-tracer datasets were used (1) continuous profiles of turbidity levels obtained from the original ASPA GUDI well tests, (2) indicator bacteria concentrations sampled discretely at both GUDI and non-GUDI wells on a monthly basis, and (3) water isotope values in precipitation and groundwater sampled discretely over short and long time resolutions. Additionally, video logs of ASPA wells were obtained and examined to visually assess well construction and casing integrity.

Turbidity is an indirect measure of suspended particulates and colloids in water, thus in groundwater, turbidity levels are controlled by source water particulate load, aquifer filtration capacity, and the degree of sedimentation occurring along subsurface flow paths. Turbidity is commonly used as a tracer for understanding recharge dynamics and microbial contamination in karst systems (e.g., Massei et al. 2006; Pronk et al. 2009; Goldscheider et al. 2010). However, there are relatively few studies that address this parameter in basaltic aquifers (e.g., Levitt et al. 2005). Nonetheless, in young, highly-permeable basalts, such as those that make up the Tafuna-Leone Plain (Stearns 1944), lava tubes and high secondary porosity from prevalent fractures may support conduit and fracture flow similar to that of karstic aquifers (Kiernan et al. 2003). While the presence or absence of turbidity is a commonly used metric in regulatory water testing worldwide, its use as a tracer for assessing recharge dynamics in high-permeability basalt aquifers remains, to the authors' knowledge, a novel approach.

Presence of short-lived endogenous or soil bacteria species in groundwater indicates lack of aquifer filtration capacity and short groundwater travel time, as *E. coli* die off rates in this environment may be greater than 50% per day (Entry and Farmer 2001; Foppen and Schijven 2006). In tropical climates, *E. coli* and other coliforms in groundwater do not necessarily signify fecal contamination as they do in temperate climates (Byappanahalli and Fujioka 1998; Byappanahalli et al. 2012). However, when detected in wells, these organisms indicate a direct and rapid connection between production well pumps and surface waters or soils, which have been found to be significant sources of *E. coli* and TC in American Samoa (Kirs et al. 2017). Bacteriological tracers have previously been applied in numerous settings for determining groundwater travel times through preferential pathways that lie at the statistically-rapid end of flow-velocity distributions (Barrell & Rowland 1979; Taylor et al. 2004; Godfrey et al. 2005).

The isotopic composition ($\delta^{18}O$ and $\delta^{2}H$) of precipitation and groundwater is commonly used to assess recharge source, elevation, or timing. Water isotopes are widely applied globally, and there are numerous examples of their application in tropical environments to better understand recharge dynamics (Scholl et al. 2002; Rhodes et al. 2006; Fackrell 2016). Potential factors that affect $\delta^{18}O$ and $\delta^{2}H$ fractionation in rainfall include the temperature-dependence of vapor-liquid fractionation, shifts in water vapor-source regions,

or progressive enrichment due to Raleigh fractionation occurring as source vapor becomes progressively more 'rained out' with increasing elevation or distance from sources (Dansgaard 1964; Rozanski et al., 1993; Gat, 1996). At sites within the intertropical convergence zone, such as the Samoan Archipelago, distinctive seasonal fractionation effects have been observed. These effects have been attributed to either seasonal shifts in water vapor source regions (Cobb et al., 2007) or variability in rainfall type. For example, in Costa Rica, Rhodes et al. (2006) found that convective storms are more prevalent in the wet-season and produce isotopically depleted rainfall, whereas dry season trade-wind showers were seen to produce more isotopically enriched rainfall. Although the direct causes of this variability probably vary from region to region, observed and predictable seasonality in precipitation isotopes allows them to be applied in this study as a seasonal-scale tracer of groundwater recharge timing. While this intertropical seasonality effect has been used before to partition hydrographs and study surface-water dynamics (e.g. Birkel et al. 2016; Calderon and Uhlenbroo 2016), its use for assessing groundwater-contaminant transit times is, to the authors' knowledge, an innovative application.

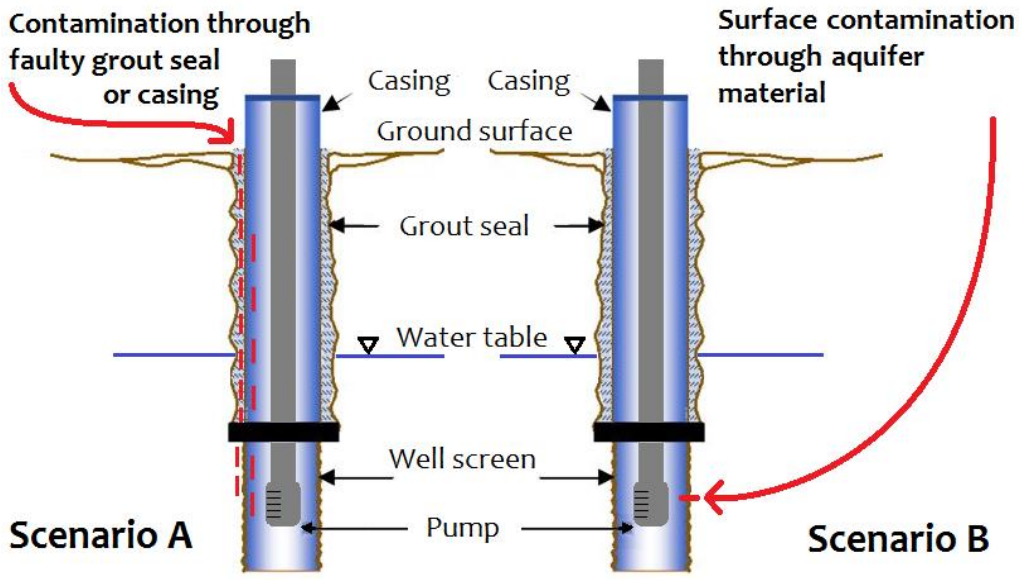

Figure 2.1: Hypothesized flow paths of surface derived contamination in GUDI wells. Scenario A shows contaminated water (*indicated by red lines*) entering a well through a poorly sealed packing or well casing, while Scenario B depicts contamination traveling to a well pump through highly permeable aquifer matrix.

2.1.1 Study Location

American Samoa encompasses the four smallest high-volcanic islands in the Samoan hot spot chain, which is located in the South Pacific about half-way between Hawaii and New Zealand (Fig. 2.2). Tutuila is the largest and most populous island in the territory, with a land area of 142 km^2 and a population density of almost 400 people/km^2. Geologically, Tutuila can be divided into two primary lithologies, the older shields and the younger Tafuna-Leone Plain. The Pleistocene age shield volcanoes comprise the bulk of the island, and consist of four merged eruptive centers that have subsequently been eroded into a steep and heavily forested ridgeline (Stearns 1944). Aquifer tests on wells in the Pleistocene unit show relatively low hydraulic conductivities (***K***). On the shields' southwestern flank, Holocene age rejuvenated volcanism later accreted the Tafuna-Leone Plain, a 30 km^2 lava delta pocketed with a number of volcanic cones and craters, and containing lava tubes and high-secondary porosity from abundant fracturing (Keating and Bolton 1992; Izuka et al. 2007).

The Tafuna-Leone Plain can be divided into the predominantly thin bedded pahoehoe lava flows of the Tafuna Unit on the eastern side and the interbedded ash and lava layers that comprise the Leone Unit on the plain's western side. While permeabilities throughout the plain are generally higher than in the Pleistocene shields, ***K*** values in the Leone Unit are generally lower than in Tafuna due to enhanced deposition of volcanic ash driven by prevailing easterly winds from vents on the central plain. Soils on the Tafuna-Leone Plain are thin and in many places on the Tafuna side, bedrock outcrops directly at ground level (Nakamura 1984).

Tutuila's climate is hot and humid throughout the year, with average temperatures around 28℃ and annual rainfall ranging between 3000 and 6000 mm/year. High rainfall rates are common since much of Tutuila's precipitation is generated from convective cells (thunderstorms) forming within the South Pacific Convergence Zone. Heavy rainfall from frequent tropical cyclones is also common during the austral summer. Although there is a wetter season, which extends from October to May and a drier season that spans June to September, prevalent rainfall occurs throughout the year (Fig. 2.3).

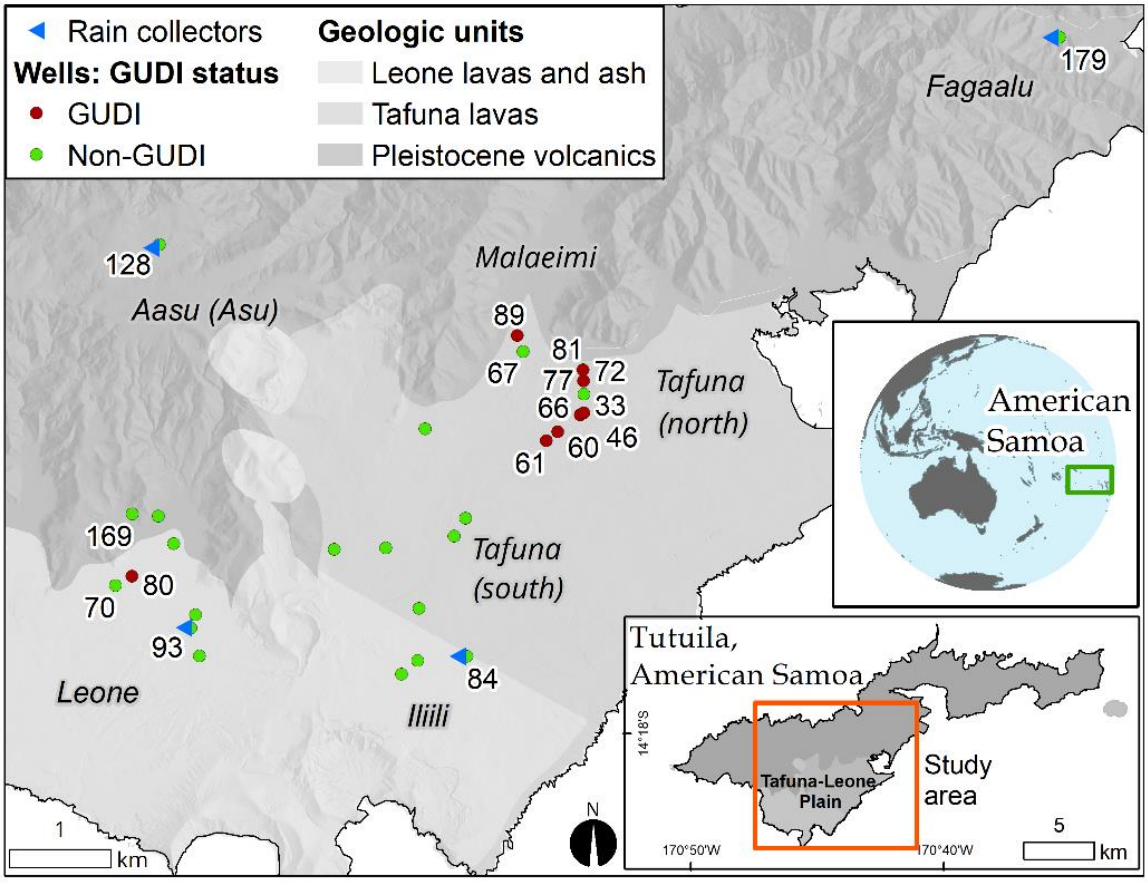

Figure 2.2: Study region, locations of municipal wells (*filled circles*), and simplified geologic units. Pertinent wells are labeled by ID number and are color coded by U.S. Environmental Protection Agency (US-EPA) determined GUDI status. Rainfall collectors were deployed at four wells and are indicated by *blue triangles*. Well field regions are also labeled. Geologic units are modified from Stearns (1944).

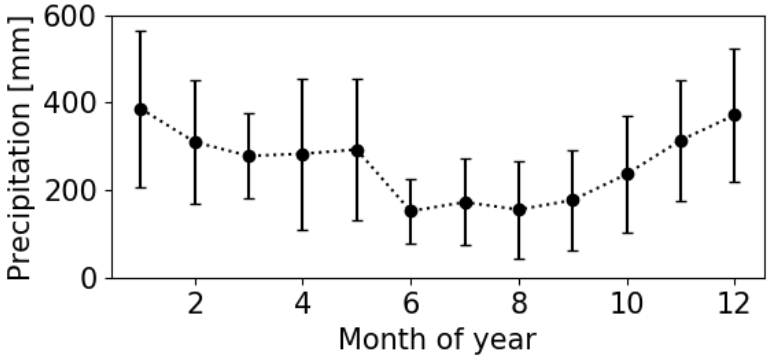

Figure 2.3: Seasonal precipitation cycle from the Pago Airport station, calculated June 1987 to May 2017. Error bars show 1σ standard deviation.

2.2 Methods

2.2.1 Turbidity, Rainfall, and Video Log Data

Turbidity and local rainfall data from GUDI well tests were provided by ASPA for this study. Between 2012 and 2016, ASPA performed a total of thirty-eight tests on wells throughout the ASPA system. These tests were conducted one well at a time, during which an instrument package consisting of an in-line Turbidimeter (Hach model 1720E) and a tipping-bucket rain gage (RainWise model 804-1011) was installed at each well site for an average test period of roughly 2 months. Additionally, discrete water samples were periodically collected and analyzed at the AS-EPA microbiology laboratory for TC and *E. coli* concentrations. However, due to low sampling resolution, these microbial measurements are not analyzed in this study. Borehole video logging was also performed by ASPA on at least ten of the tested wells. Reports stored in ASPA files document methodology, and resulting GUDI status determinations for each well studied (e.g., Vold et al. 2013).

For this study, additional analysis of raw ASPA turbidly data was performed by filtering one-minute resolution turbidimeter measurements with a 1-hour rolling-median pass filter and smoothing with a Gaussian routine (*scipy.signal.general_gaussian*, https://scipy.org/) to remove prevalent high-frequency spikes present in many of the datasets. These short duration spikes were assumed be an artifact of bubbles within the supply line (Mauga 2016). An automated peak detection routine (*peakdet*, https://gist.github.com/endolith/250860) was then applied to identify the position of significant turbidity peaks. The start and end of each peak was defined as the point where turbidity levels departed significantly from a baseline turbidity value that was statistically determined for each dataset, except when a subsequent peak occurred before a previous peak had fully decayed. In this case, the inflection point between the two peaks was defined as both

the end of the first and the start of the second peak. Rainfall data from tipping-bucket gauges were consolidated into hourly totals and filled in with daily rainfall totals from the nearby Pago Pago Airport weather station (https://www.weather.gov/ppg/) where rainfall data at the well was missing. Heavy rainfall events were defined at the midpoint of any three-hour rolling-sum time-window with > 25 mm (1 inch) of recorded rainfall (Glickman 2000). Rainfall and turbidity peak data was plotted and manually inspected to define rain-event related turbidity peaks that occurred within 7 days of a heavy-rainfall event. Turbidity peaks not preceded by a heavy-rainfall event, or rainfall events not antecedent of a turbidity peak were ignored. Once rain-event turbidity-peak pairs were identified, the peak duration, time between rain event and start of the peak, and the time between rain event and maximum value of the peak were calculated for each event. For this study, borehole video logs were also reviewed to document depth to water, depth of well, casing depth, and any issues with casing integrity.

2.2.2 Indicator Bacteria on Annual Scales

Indicator bacteria (TC and *E. coli*) were examined to assess microbial water quality variability in Tutuila's groundwater throughout different seasons and during selected rainfall events. Raw production well-water was regularly sampled at monthly intervals from well sample taps at four GUDI wells in the North Tafuna (N. Tafuna) well field and four non-GUDI wells throughout the island during the period spanning April 2016 and September 2017. Some additional samples were also collected during or after heavy rain events to ensure these conditions were well represented in the dataset. All microbial samples were collected in 100 ml sterilized plastic containers and cooled for transport to the laboratory at the American Samoa Community College (ASCC) for microbiological analyses. In the ASCC laboratory, Colilert®-18 kits and Quanti-Trays®/2000 (IDEXX Laboratories Inc., Westbrook, ME) were used to determine concentrations and 95% confidence intervals of TC and E. *coli* bacteria as most probable number (MPN) per 100 ml according to the manufacturer's protocol. Time between sample collection and analysis never exceeded 6 hours.

2.2.3 Water Isotopes in Precipitation and Groundwater

Water isotope samples from precipitation and groundwater were collected at two distinct time resolutions. Annual variation was assessed through water isotope samples collected on a monthly basis for a three-year sampling period from both production wells and rainfall collectors located throughout the island. Precipitation was collected in cumulative precipitation collectors (CPC's) following the design used in Scholl et al. (1996). Collectors contained a 1-2 cm thick layer of high-purity mineral oil that floated on top of and prevented evaporation from collected water. All water was removed from collectors during sampling, thus each monthly sample represented the integrated water isotope composition of all precipitation falling during the whole month. Four collectors were deployed thought Tutuila, at sites representative of various conditions that might affect precipitation isotope fractionation such as elevation or location. After 2 years, it was found that there was little

isotopic variation between collection sites, therefore sampling from three of the collectors was discontinued. Sampling continued for a total of three years at the collector located on the Tafuna side of the Plain, and the water isotope composition observed at this site was presumed to be representative of all precipitation within the study area. Water isotope composition of groundwater was assessed through samples collected each month over the three-year period from selected GUDI and non-GUDI production wells. Groundwater was always sampled from production well taps when well pumps were running.

To assess rainfall response at short time scales, a high-resolution time-series of water isotope samples was also collected at five GUDI wells and two non-GUDI wells during a three-week rainfall-event period in April, 2016. Water levels in each well were also measured through sounding tubes during sample collection with an electric water level indicator. Precipitation from just a single 3-day storm event at the beginning of the three-week period was collected separately from the precipitation collected for monthly sampling. Precipitation totals during this period were determined with rainfall data recorded by a weather station located at the nearby community college in Malaeimi Village (ASCC 2018), which is located about 1 km northwest of the N. Tafuna well field.

All water isotope samples were collected in 20 ml glass vials with no headspace, and were analyzed for $\delta^{18}O$ and $\delta^{2}H$ of water in a Picarro brand Cavity Ring-Down Spectrometer (L1102-i Isotopic Liquid Water Analyzer) at the University of Hawaii Stable Isotope Biogeochemistry Laboratory. Analytical uncertainty averaged ±0.07‰ for $\delta^{18}O$ and ±0.38‰ for $\delta^{2}H$, and was assessed through computing the standard error of the estimate of duplicate samples, which made up about 15% of the dataset. All water isotope values referred to in this work are expressed in permil notation (‰) and are relative to the international standard V-SMOW.

2.3 Results

2.3.1 Results: Groundwater Turbidity and Response to Rainfall

Clearly defined rainfall-event related turbidity peaks up to 7 NTU were detected in all of the N. Tafuna wells, (Wells 33, 60, 61, 66, 72, 77, and 81), which are mostly designated as GUDI wells. On average, turbidity peaks in these wells generally had a sharp onset at 17± 11 hours after rainfall events, reached their maximum value around 36 ± 21 hours, and then trailed off with a subsequent exponential decay (Fig. 2.4a). Observed turbidity peaks lasted for a duration of 36 to 265 hours, although the length of many peaks was cut short when a subsequent peak interfered with the decay of the preceding peak (Table 2.1). Turbidity in most non-GUDI designated wells remained stable at very low levels (Fig. 2.4b), except in some cases where factors unrelated to rainfall seemed to stir up turbidity, such as daily cycles of pump activation. Also, Well 77 (located between wells 33 and 81) was originally designated

as the only non-GUDI well in N. Tafuna. However, turbidity data from Well 77 showed a well-defined 2 NTU magnitude peak, which was comparable to those in the other N. Tafuna wells (Fig. 2.4c). No other significant rain-event turbidity peak pairs were detected in any non-GUDI wells that are not specifically discussed in this section or noted in Table 2.1.

It should also be noted that the bimodal US-EPA designation of GUDI or non-GUDI for Tutuila's wells does not necessarily reflect the spectrum of variability in aquifer and well construction conditions observed in the field. While most of the GUDI wells show a similar response to rainfall, and most of the designated non-GUDI wells show little to no response, there are a number of outliers. Notable outliers include:

- Well 80 is the only GUDI well in Leone and shows a very subdued turbidity response.
- Wells 77 and 67 are located in the N. Tafuna and Malaeimi well fields and show a similar turbidity response to GUDI wells, yet are both designated as non-GUDI.
- Well 169 is designated as non-GUDI, but was found through video logging to have a significant flaw in the casing integrity.

The Malaeimi well field only has two active wells, GUDI Well 89, and non-GUDI Well 67. Turbidity data in both of these wells showed peaks that were less distinctive and had lower magnitudes than peaks in the N. Tafuna wells (Fig. 2.4d). The start of peaks occurred on similar timescales, within 4 to 13 hours after rain events, but in Well 67 peak maximums did not occur for roughly 3 days after the event. Unfortunately, only one peak was captured during the Well 89 study, and it appears that the turbidimeter was not operating correctly until just before this peak.

Only one well (Well 80) in the westerly Leone well field, and within the more ash-rich Leone Geologic Unit, was originally designated as a GUDI well. However, the turbidity response to rainfall at Well 80 was dissimilar to turbidity peaks observed in other GUDI wells, as it had a lower magnitude, was more dome shaped, and occurred more slowly (mean of 85 hours to peak maximum) than peaks in N. Tafuna wells (Fig. 2.4e). The most dramatic turbidity response observed in all profiles was in non-GUDI Leone Well 169, which had the highest maximum turbidity value (25 NTU), the shortest response time (3 hrs.), and the shortest peak duration (15 hrs.) of any well that was analyzed (Fig. 2.4f). This observation alone is enigmatic, as Well 169 was designated as non-GUDI, had minimal TC and no *E. coli* detections during the test period, is located far from other GUDI wells, and lies within the Pleistocene age rocks that have much lower permeabilities than the Tafuna lavas (Izuka et al. 2007). However, analysis of the borehole video log for Well 169 clearly shows a hole in the casing at 12.5 m below ground surface. This observation is discussed in greater detail in section 2.4.1.2.

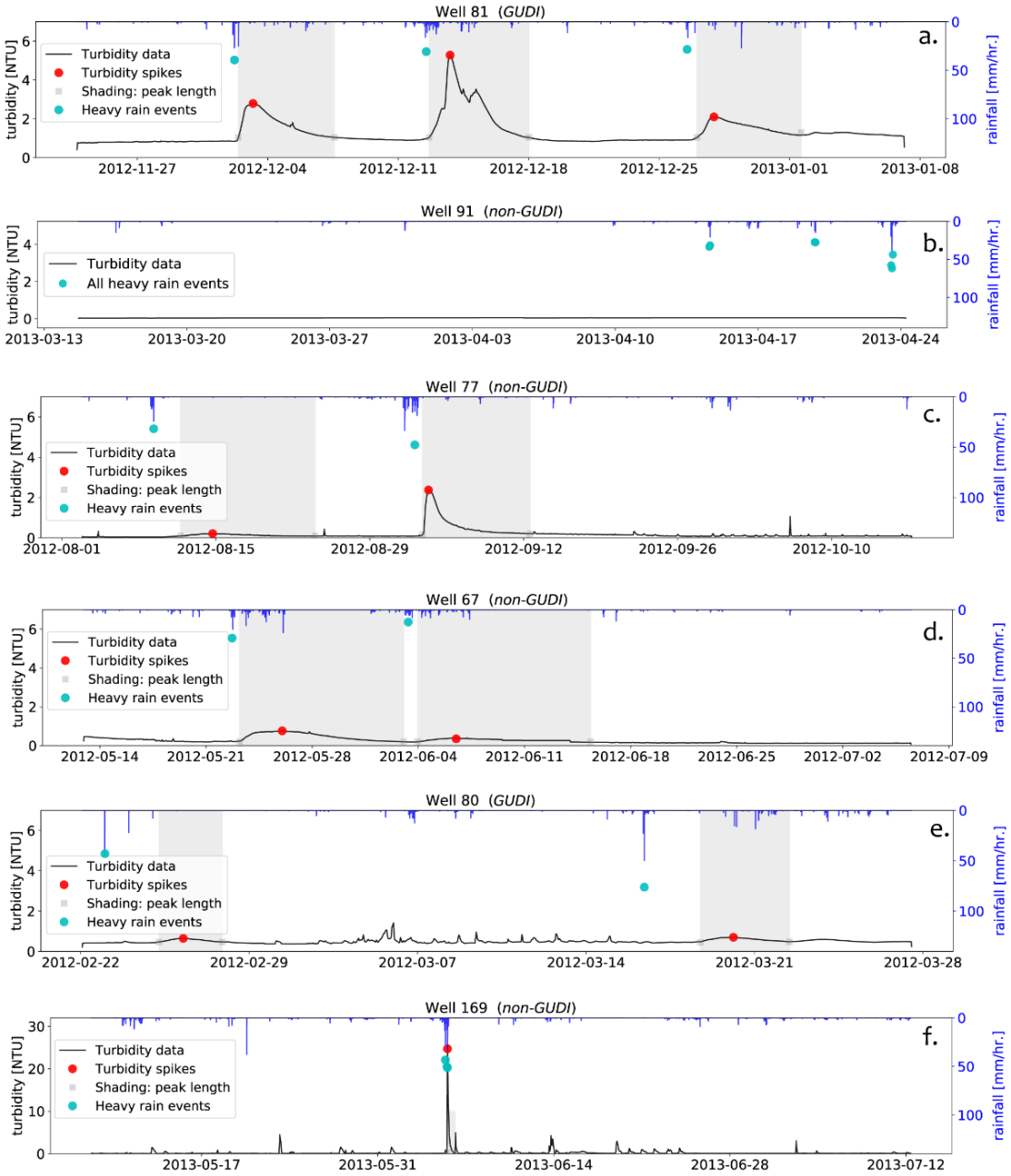

Figure 2.4: Selected ASPA GUDI well tests showing processed turbidity profiles (black lines) and rainfall (blue bars). Turbidity peaks (red dots) that correlate with preceding heavy-rainfall events (blue dots) are shown, and grey shaded fields represent durations of turbidity peaks. (a) Data from Well 81 shows the archetypical rainfall – turbidity peak response generally observed at all wells in the Tafuna wellfield. (b) Well 91 exemplifies the lack of response typical in most non-GUDI wells. (c and d) Well 67 and 77, despite being classified as non-GUDI, these wells show rainfall – turbidity responses similar to Tafuna GUDI wells, albeit subdued in magnitude and duration. (d) Well 80, located in Leone, is classified by AS-EPA as GUDI, but shows a subdued rainfall response of very low magnitude. (e) Well 169 is unique amongst all wells studied, as it is designated non-GUDI, but shows a dramatic response due to a hole in the casing (observed during a video log).

Table 2.1: Relevant statistics averaged across all rainfall-event turbidity peak pairs observed during continuous turbidity profiles. “Response to peak” indicates time between the defined rainfall event and the time of the maximum turbidity value. “Response to peak start” indicates time between the defined rainfall event and the point where turbidity departed from the baseline value. Wells are grouped by well field and only N. Tafuna wells are summarized with wellfield averages and 1σ standard deviations (S.D.) (in parentheses), as other well fields have fewer wells and more variability in response to rainfall.

N. Tafuna Wells	Length of spike [hrs.]	Maximum Turbidity [NTU]	Response to peak [hrs.]	Response to peak start [hrs.]	Number of peaks recorded
Well 33 (GUDI)*	36	1.1	26	13	3
Well 60 (GUDI)	35	1.5	33	22	3
Well 61 (GUDI)	37	5.4	12	7	3
Well 66 (GUDI)	86	2.2	37	15	3
Well 72 (GUDI)	127	6.2	42	16	3
Well 77 (non-GUDI)	265	2.4	79	38	2
Well 81 (GUDI)	129	5.3	30	7	3
Average and S.D.	**102 ± (83)**	**3 ± (2)**	**37 ± (21)**	**17 ± (11)**	**20 Total**
Malaeimi Wells					
Well 89 (GUDI)	119	1.1	18	4	1
Well 67 (non-GUDI)	267	0.8	78	13	2
Leone wells					
Well 80 (GUDI)	76	1	84	55	2
Well 70 (non-GUDI)	130	0.04	87	40	1
Well 169 (non-GUDI)**	15	25	4	3	1

* Note GUDI designation was previously determined by ASPA, not during this study

** Well 169 has a hole in casing, but was previously designated as non-GUDI

2.3.2 Results: Indicator Bacteria in GUDI and non-GUDI Wells.

Of the 69 microbial samples taken during this study at GUDI wells over the period April 2016 to September 2017, about 95% and 85% tested positive for TC and *E. coli*, respectively. In contrast, TC and *E. coli* detection rates in the 50 samples taken at non-GUDI wells were 28% and 0%, respectively. Concentrations of both TC and *E. coli* were highly variable in GUDI wells (< 1 to > 2419.6 MPN/100 ml), and when detected in non-GUDI wells, TC concentrations were always less than 10 MPN/100 ml. Correlation between TC and *E. coli* was moderate (r^2 of 0.52 for all samples).

Microbial samples were taken during rainy periods and dry periods for about a year and a half on a monthly basis (Fig. 2.5). Three additional sample sets were collected during

targeted rainy periods to ensure all climatic conditions were well represented in the dataset. To find the most likely transport times for surface living bacteria detected at well pumps, correlation coefficients between *E. coli* concentrations and preceding rainfall totals calculated at various time-lags (defined as the number of hours before each sample was taken) were determined. This was accomplished for each of the four regularly sampled GUDI wells by calculating the least-squares coefficient of determination (r^2) between sampled *E. coli* concentrations and an array of 12-hour rainfall totals at varying time-lags prior to the documented *E. coli* sample time. The array of time-lag values was created by summing all rainfall within a 12-hour window for every possible time-lag (on an hourly step), starting 168 hours (7 days) before and leading up to the time each sample was taken. Rainfall data was obtained from a weather station located at the nearby American Samoa Community College in Malaeimi Village (ASCC 2018). In Fig. 2.6 (top row), r^2 values are shown as the dependent variable, with the time-lag used to calculate 12-hour rainfall totals serving as the independent variable. Figure 2.6 (bottom row) shows the correlation between *E. coli* concentrations and the 12-hour rainfall totals at the best-fitting (meaning maximum r^2 value) time-lag window for each well.

Interestingly, there were two specific time-lags that consistently resulted in high correlation between rainfall and *E. coli* concentrations. Rainfall windows centered around 18 to 19 hours before sampling time produced high-correlations in three of the wells (Wells 33, 89, and 81) and in all four of the wells, a second correlation peak somewhere around 45 to 65 hours before sampling time was also observed. For time-lags preceding these local maxima, the correlation tended to drop off, except at Well 60, where the r^2 value started to plateau around 0.9. Well 60 was also the well with the least number of samples. This analysis suggests a large proportion of the variability in these well's *E. coli* concentrations can be explained by the amount of rainfall occurring either the day before (18 to 19 hours) or a couple of days before (45 to 65 hours) sampling. The best-fitting travel times for the first of the two *E. coli* – rainfall correlation peaks are similar to the travel times observed between rainfall and the start of turbidity peaks in the N. Tafuna wells (17 ± 11 hours). Both of these processes would be expected to represent statistically extreme groundwater flowpaths. However, it is unclear what the correlation peaks at longer-time lags (45 to 65 hours) represent. The maximum values of turbidity breakthrough curves (37± 21 hours), which should represent average travel time for turbidity, occur at a slightly shorter time lag. Nonetheless, in individual wells, *E. coli* – rainfall peak timing and turbidity breakthrough timing do not show an explicit match, which may be due to a lack of microbial sample density, as well as having only a limited number of rain events represented in each turbidity profile.

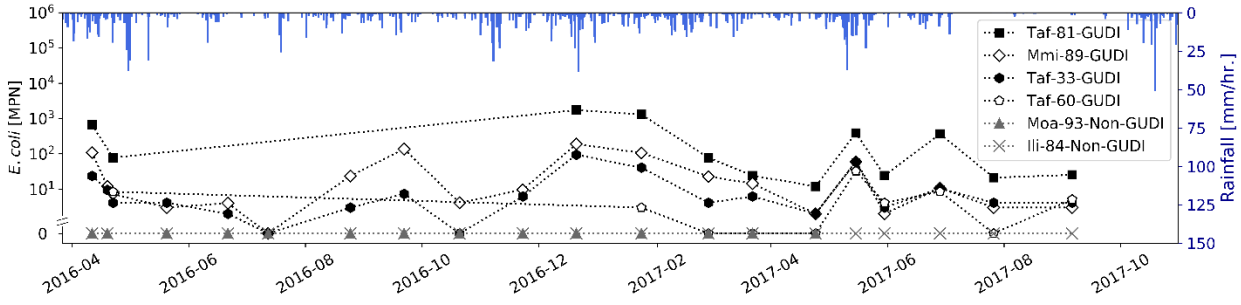

Figure 2.5: *E. coli* concentrations from monthly microbial sampling at GUDI and non-GUDI wells plotted with hourly rainfall totals from ASCC weather station. Note lines connecting sample points are shown for visual continuity only, and are not intended to infer concentrations between points.

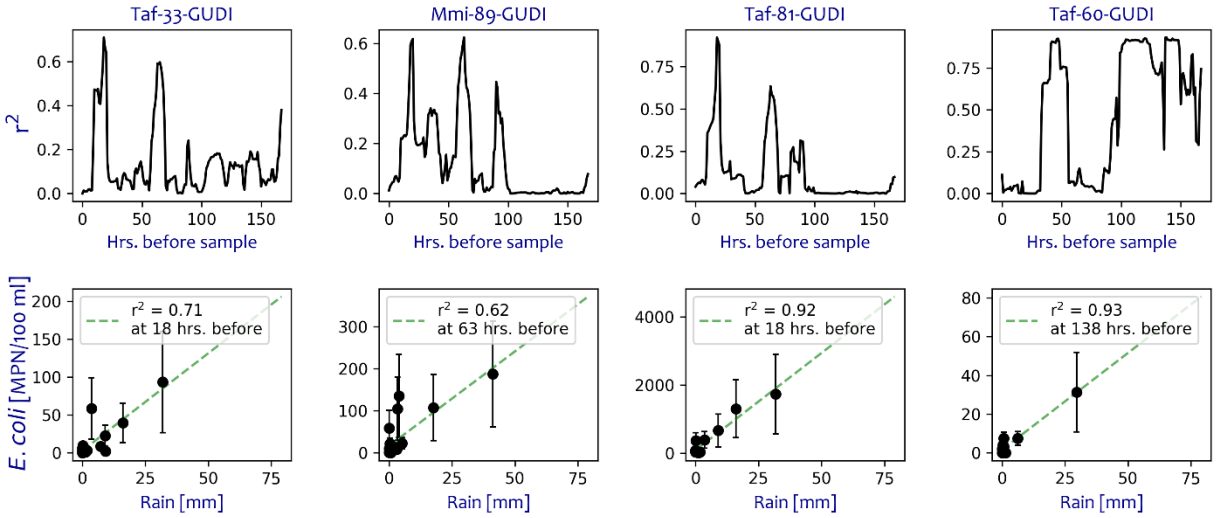

Figure 2.6: Correlation analysis between *E. coli* concentrations and rainfall totals used to estimate microbial travel time in groundwater. Top row of plots shows variation in r^2 (y axis) as 12-hour rainfall totals are calculated at various the time-lags prior to the sample time (x axis). Bottom row shows scatter plots of *E. coli* concentrations vs. the rainfall total calculated at the best-fitting time-lag (maximum r^2) from the plots directly above. *Green dashed lines* represent least-squares regressions, and the best-fit time lag in hours before sample time, and resulting r^2 value at that time lag, are noted in the plot legends. Error bars represent 95% confidence intervals for MPN calculations and p-values for correlation analysis were all below 0.0003.

2.3.3. Results: Water Isotopes in Precipitation and Groundwater

2.3.3.1 Seasonal $\delta^{18}O$ and $\delta^{2}H$ Response

Three years of monthly rainfall sampling revealed strong, cyclical, and seasonal variation in water oxygen and hydrogen isotope compositions (Fig. 2.7). Precipitation $\delta^{2}H$ and $\delta^{18}O$ values during the austral winter were enriched in heavy isotopes, ranging up to +8‰ and -1 ‰, respectively, and were much more depleted in the austral summer, ranging down to -55‰ and -8‰, respectively. In the fall and spring seasons, precipitation $\delta^{2}H$ and $\delta^{18}O$ values transitioned between the extreme values recorded closer to the solstices. In contrast, monthly sampling at both GUDI and non-GUDI wells over the 3-year period showed limited variation in groundwater isotope compositions, which were generally close to the volume-weighted average-annual composition of precipitation (Table 2.2), and ranged between -3.5‰ and -5.6 ‰ for $\delta^{18}O$ and -16.1‰ and -24.5 ‰ for $\delta^{2}H$. While the causes and patterns of observed $\delta^{2}H$ and $\delta^{18}O$ variation remain beyond the scope of this work, the pertinent implication to this study is that during months where the isotopic composition of precipitation is distinct from that of groundwater, $\delta^{2}H$ and $\delta^{18}O$ values in well samples can be used to determine the presence and even quantify the proportion of recently recharged water.

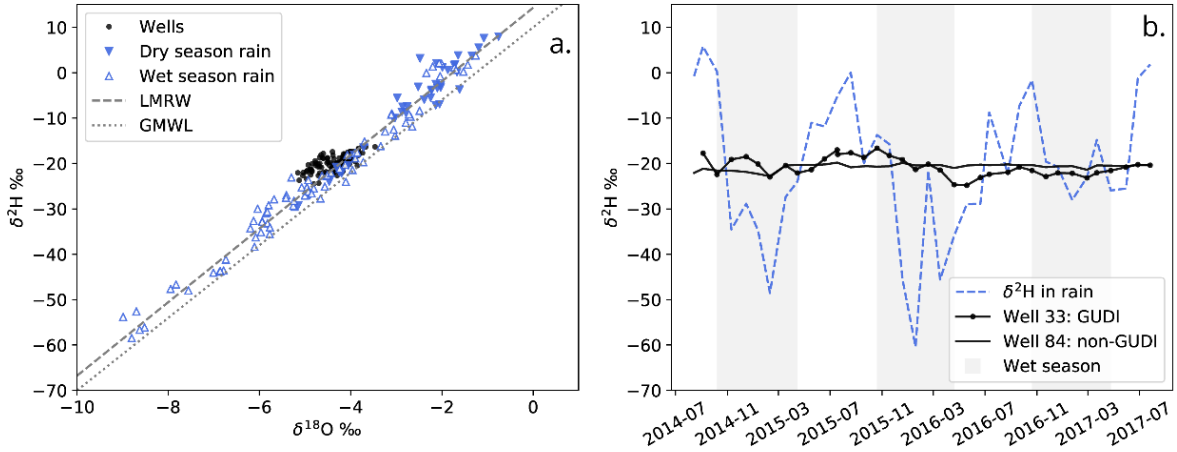

Figure 2.7: Water isotope values from rainfall collectors and groundwater wells. Dual-isotope diagram of $\delta^{2}H$ and $\delta^{18}O$ values (panel a), with regression through all rainfall samples showing the Local Meteoric Water Line (LMWR) plotted as dashed line, with the Global Meteoric Water Line (GMWR) shown as dotted line for reference. Seasonal variation (panel b) of water isotope ($\delta^{2}H$) values in precipitation at the Iliili rainfall collector (*dashed line)* and in groundwater at selected wells (*solid lines*). Well 33 showed the most variation and Well 84 the least variation of all sampled wells. Grey shaded regions indicate the wet season. Note, $\delta^{18}O$ values (not shown) followed the same pattern, and analytical uncertainties plot smaller than the symbol size.

2.3.3.2 Event-Scale $\delta^{18}O$ and $\delta^{2}H$ Response

Isotope tracers were most useful in this study for assessing recharge dynamics at a rain-event scale time resolution. Isotope samples and water levels collected roughly every other day from three GUDI and two non-GUDI wells formed a two-week long event-scale time-series where the effects of multiple heavy rainfall events and a subsequent period of drier weather could be observed (Fig. 2.8). The first day of well sampling took place as the most pronounced multi-day heavy-rain event was occurring. Two additional GUDI wells, 81 and 72 were sampled at a lower frequency, only once during the wet portion of the sampling period and once afterwards. These wells ended up showing the largest water isotope variations, and unfortunately their pre-rain event water isotope composition was not sampled. Instead, the pre-rain event isotopic compositions at Wells 81 and 72 was assumed to be equal to their measured values taken near the end of the sampling period. This assumption was considered reasonable as the substituted compositions were at most within 5% RPD of the pre-rain event compositions of Wells 33 and 46, which are located within 400 m of Wells 81 and 72.

The storm event precipitation was collected at Fagaalu Village, located about 6 km to the east of Tafuna, over a three-day period starting before the initial heavy rainfall event and ending as rainfall rates were declining. Additionally, a rain collector in the village of Iliili, located about 5 km to the southwest of N. Tafuna, was deployed for the entire month of April and integrated all precipitation that fell within the month. Both of these precipitation samples had isotopic compositions (-5.9‰ and -35.3‰ (storm event) and -5.8‰ and -34.1‰ (monthly sample) for $\delta^{18}O$ and $\delta^{2}H$, respectively) that were distinct from average annual values of Tutuila's groundwater.

At four of the five GUDI wells, water isotope values generally started around -4.5‰ ($\delta^{18}O$) and --22.5‰ ($\delta^{2}H$), which are near but slightly depleted relative to the average annual composition of groundwater (Table 2.2). Within the first week of sampling, $\delta^{18}O$ and $\delta^{2}H$ values dropped towards the composition of storm-event precipitation, with values at Well 81 reaching -5.3‰ ($\delta^{18}O$) and -28.3‰ ($\delta^{2}H$). After the initial rainy portion of the sampling period, isotope compositions at the GUDI wells moved back towards the average groundwater composition, and were seen to dip slightly again as a final rain event occurred before the last day of the sampling period. On the other hand, water isotope compositions at the two sampled non-GUDI wells remained consistent throughout the sampling period. Water isotope values in these wells started and remained at a less depleted value than in the N. Tafuna wells. However, by the end of the time-series a very slight drop in $\delta^{18}O$ and $\delta^{2}H$ composition (on the order of 0.5‰ to 1‰ in $\delta^{2}H$) was observed, which may indicate a delayed response to the recharge event. Additionally, Well 89, classified as GUDI and located almost 1 km from the center of the N. Tafuna wellfield, showed little response to precipitation, and displayed a subdued response comparable to the two non-GUDI wells. Water isotope magnitudes in Well 89 were also similar to the non-GUDI wells, in that the starting and ending isotopic

compositions, more closely matched the average annual groundwater $\delta^{18}O$ and $\delta^{2}H$ composition.

Water levels were also taken during each sampling, and all wells showed a significant though somewhat delayed response to rainfall, with water levels in the GUDI wells showing between 2 and 5.5 m of increase by the end of the rainy period (Fig. 2.9). At these wells, maximum water level measurements corresponded to times where minimum (most similar to recent rainfall) $\delta^{18}O$ and $\delta^{2}H$ values were observed. In non-GUDI wells a more subdued water level increase was recorded, up to about 1.5 m of rise, with notable differences from the GUDI wells being a slightly slower response, and also a much less precipitous and slower return back towards pre-event levels after the rainfall event had ceased. Since water levels are dependent on local hydrogeologic factors such as regional aquifer heads and aquifer connectivity, they are not simply a function of a volumetric addition of recharge. Nonetheless, these results show how heavy rainfalls significantly affect water availability in this region's aquifers.

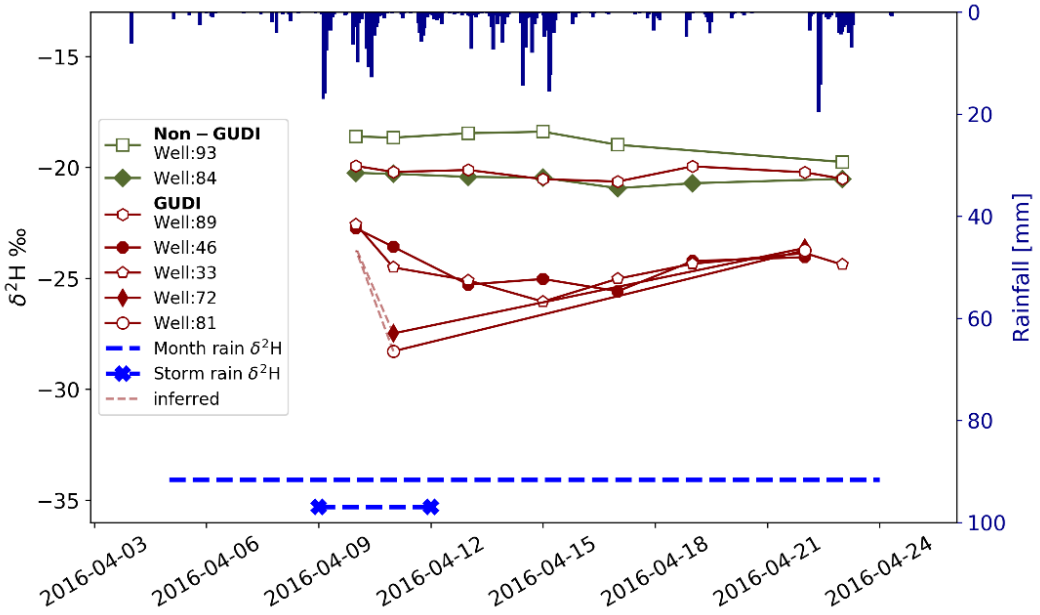

Figure 2.8: Water isotope values ($\delta^{2}H$) from groundwater wells (*red and green lines*) and precipitation (*dark blue bars*) over a three-week heavy rain-event period. Wells were sampled at discrete times, whereas precipitation samples represent the volume weighted integration of all rain falling throughout two multi-day collection periods; (1) a 3-day period spanning the initial heavy rain event (*dashed line with blue X*) and (2) over the entire month of April (*dashed line with no X*). Note that analytical uncertainties plot at roughly the same magnitude as the symbol size, and only $\delta^{2}H$ values are illustrated since $\delta^{18}O$ values show similar patterns.

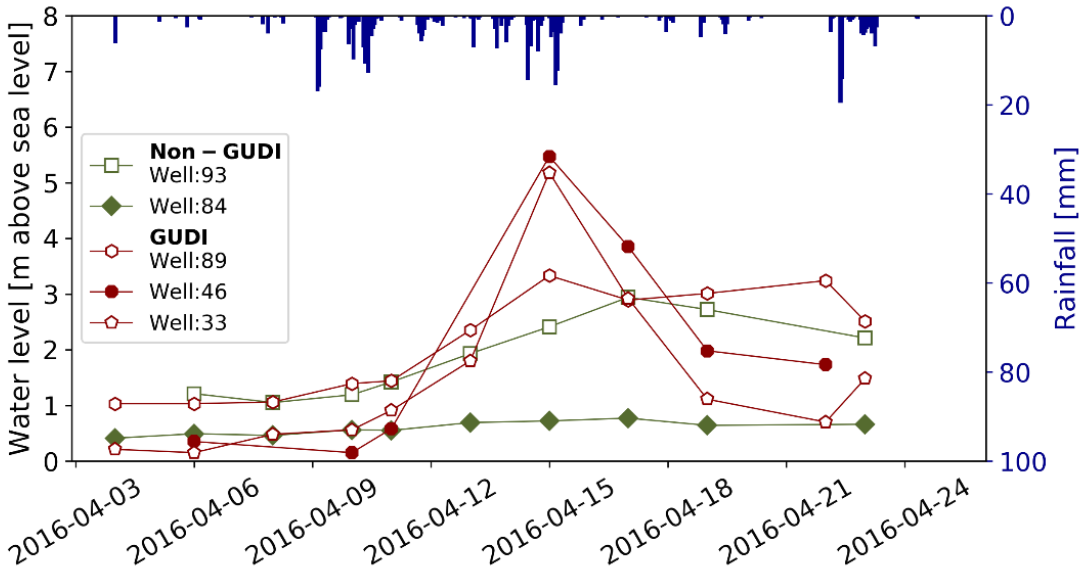

Figure 2.9: Water level variation at three GUDI and two non-GUDI wells measured concurrently with water isotope samples taken during the three-week heavy rain-event period.

Table 2.2: Average annual δ18O and δ2H values and 1σ S.D. (in parentheses) as measured through monthly sampling of wells and precipitation collectors. Precipitation values are volume weighted to amount of water collected each month. Note, for volume weighted samples 1σ S.D. is calculated for unweighted data to show the degree of seasonal variability.

Site	$\delta^{18}O$ [‰]	$\delta^{2}H$ [‰]
Precipitation Collectors: Volume Weighted Averages		
Aasu	-4.61 (1.98)	-22.07 (16.52)
Fagaalu	-5.01 (2.02)	-26.38 (16.2)
Iliili	-4.93 (1.87)	-25.96 (15.48)
Leone	-4.94 (1.91)	-25.99 (15.58)
All collector average	**-4.87 (1.95)**	**-25.10 (15.95)**
Production Wells: Averages		
Aasu 128	-4.22 (0.34)	-18.52 (1.00)
Fagaalu 179	-4.45 (0.29)	-21.18 (0.83)
Iliili 84	-4.26 (0.29)	-20.43 (0.67)
Malaeimi 89	-4.18 (0.25)	-19.06 (1.19)
Leone 93	-4.23 (0.22)	-20.21 (1.41)
Tafuna 33	-4.30 (0.31)	-20.42 (2.05)
All well average	**-4.27 (0.28)**	**-19.97 (1.19)**

2.4 Discussion

2.4.1 Expected Groundwater Travel Times

Comparing observed travel times from tracer based methods with expected travel times in aquifer material or through faulty casings allowed determination of which contamination mechanism is most likely. Expected travel times for each mechanism were estimated by assessing previously published information, as well as examination of turbidity and video log observations, as detailed below.

2.4.1.1 Travel Time Through Aquifer Material

Overlooking dispersion effects, subsurface travel time is controlled by two primary factors, the distance traveled and the average rate at which water moves along the flow path. Thus, the depth of the pump at any given production well represents a minimum travel distance, with much longer distances possible. While rates of travel through the Tafuna-Leone Aquifers are probably variable, reasonable estimates of this parameter can be found in reported values for general cases of conduit flow, a likely flow mechanism in young basalt aquifers (Kiernan et al. 2003).

Kresic (2006) summarized and reported numerous measurements of groundwater velocity in karst terrains thought to be influenced by conduit flow. These estimates ranged between 400 to 2500 m/day and a typical average value of 716 m/day was suggested, as taken from 43 estimates at a West Virginia karst site. Although no reported measurements of groundwater velocity in aquifers of the Tafuna-Leone Plain have been found, Bentley (1975) reported an average transmissivity (***T***) value of 1,149 m^2/day from pump tests of Tafuna area wells, and, Izuka et al. (2007) reported horizontal hydraulic conductivity (***K***) values specific to the Tafuna and Leone sides of the Plain of 945 m/day and 396 m/day, respectively, which were developed through calibration of a numerical model. Note also that these values are based on properties of the saturated zone whereas there exists scant information about the typically 20 to 30 m thick unsaturated zone, which like the saturated aquifer, is composed primarily of fractured basalts. A lack of information regarding matrix porosity, hydraulic gradients near pumping wells, and properties of the unsaturated zone precludes direct calculation of groundwater velocities using ***T*** or ***K*** values. However, the magnitudes of these values support the conclusion that groundwater velocities through the Tafuna side of the Plain are generally very high, and may be reasonably approximated with observed values from other conduit flow systems.

Expected groundwater travel times in the Tafuna-Leone Plain were approximated by multiplying groundwater velocities consistent with those suggested by Kresic (2006) (716 m/day) with flow distances through the Plain. Because groundwater infiltrates over an area, as opposed to a single point location, the distance recharge water travels is not a discrete number. Another complicating factor in this setting is the potential for groundwater to move through preferential pathways whose locations, conveyance rate, and prevalence of openings

is uncertain. The most reliable information regarding where water infiltrates in the Tafuna-Leone Plain was produced by Izuka et al. (2007), whereas their MODFLOW model applied the MODPATH particle tracking code to delineate areas contributing to recharge, or capture zones, for each well. If it is assumed that recharge to each well occurs only within this zone, that the actual well pumping rates are equivalent to those used in the Izuka et al., model, that the tracers used in this study (turbidity, soil bacteria, and rainfall) occur uniformly across the landscape, and that the likely heterogeneity of preferential pathways exists at a scale where openings are well distributed throughout the capture zone, then the distance parameter can be conceptualized as a distribution of distances between the well and all points throughout the capture zone. To represent this distribution, a 10 m grid of points was overlaid within each well's capture zone and the straight line distance from each point to the bottom of the well was calculated (Fig. 2.10). By dividing each of these distances by an estimated groundwater velocity from conduit flow systems, a distribution of estimated travel times was approximated (Table 2.3). Expected groundwater travel times from Table 2.3 are reasonably consistent with observed turbidity travel times in Table 2.1, which suggests overly-permeable aquifer material, as opposed to faulty well casings, is the more likely mechanism of contamination in the N. Tafuna wells.

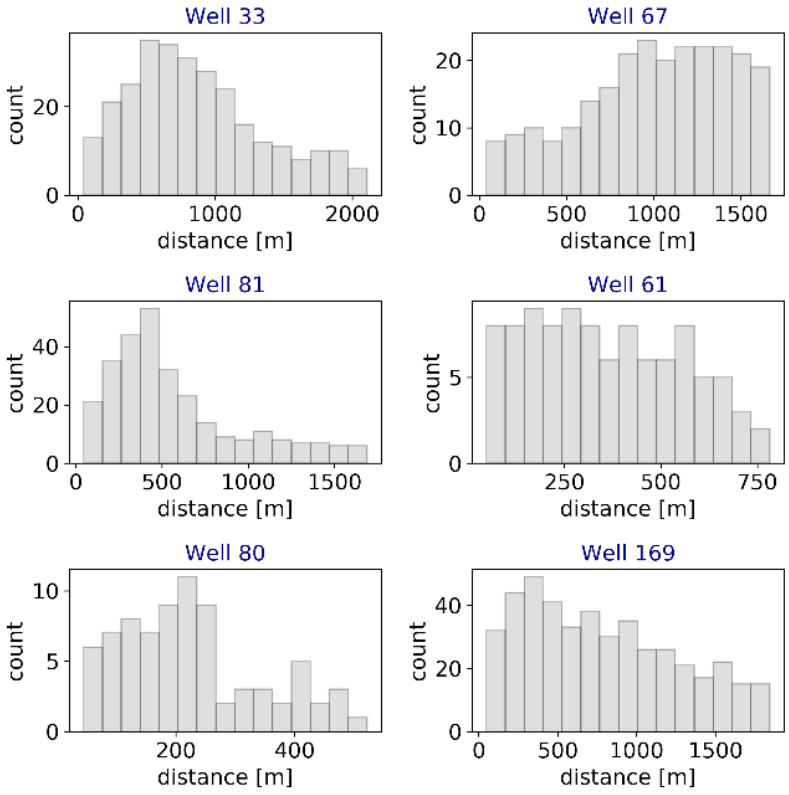

Figure 2.10: Histograms showing the distribution of distances from gridded points throughout capture zones to well pump locations for selected wells.

Table 2.3: Averages and standard deviations (in parentheses) of calculated travel distances from each well to all gridded points within each well's capture zone, and estimated average travel times derived via dividing travel distances by constant groundwater velocities taken from Izuka et al. (2007) and Kressic (2006). Travel time standard deviations (in parentheses) are propagated from travel distance standard deviations (SD).

N Tafuna Wells	Average travel distance [m]	Travel time via Kresic (2006) velocities [hrs.]**
Well 33 (GUDI)*	872 (494)	29 (16)
Well 60 (GUDI)	359 (188)	12 (6)
Well 61 (GUDI)	362 (192)	12 (6)
Well 66 (GUDI)	882 (501)	29 (16)
Well 72 (GUDI)	634 (425)	21 (14)
Well 77 (non-GUDI)	724 (461)	24 (15)
Well 81 (GUDI)	576 (388)	19 (13)
Average and SD	**-**	**21 (12)**
Malaeimi Wells		
Well 89 (GUDI)	847 (401)	28 (13)
Well 67 (non-GUDI)	995 (424)	33 (14)
Average and SD	**-**	**30 (13)**
Leone wells		
Well 80 (GUDI)	227 (117)	7 (3)
Well 70 (non-GUDI)	294 (166)	9 (5)
Well 169 (non-GUDI)**	788 (480)	26 (16)
Average and SD	**-**	**14 (8)**

* Izuka et al. (2007) velocities were 473 m/day for Tafuna/Malaeimi and 198 m/day for Leone wells ** Kressic (2006) velocity used was 716 m/day

2.4.1.2 Travel Time Through a Compromised Casing

The alternate hypothesis to contamination via overly-permeable aquifer material is that surface water travels down compromised casings or through preferential flow paths in the well packing material. In this scenario, maximum travel distance would be the pump depth. The velocity of water cascading down a well bore would be rapid, although this mechanism could still be subject to slower velocities while water percolates through the subsurface or well packing to the depth of a casing breach. Despite uncertainty in aquifer flow path travel-time estimates from section 4.1.1, it is reasonable to assume that surface water traveling through aquifer material will take significantly longer to reach a well pump than surface water traveling through and down a compromised well casing. Fortuitously, this assumption can be validated here by examining the observed turbidity response in Well 169, where a hole in the casing was observed on video during a heavy rainfall event.

In the borehole video log performed on Well 169, water could clearly be seen cascading through a less than 2 cm wide hole in the casing, because the logging was coincidentally performed during a heavy-rain event (Fig. 2.11). Upon review of all ten borehole logs provided by ASPA, only Well 169 was observed to have a casing break with active leakage. Although it is unknown if rain events occurred during video logging of other wells, the turbidity profile for Well 169 (conducted a year prior to the video log) nonetheless shows a distinctive and rapid response to the single heavy rain event recorded during the GUDI test. Within 3 hours of rainfall, a large turbidity peak was initiated, peaked within 4 hours, and returned back to baseline in 15 hours. This peak was also the highest maximum turbidity value (25 NTU) observed in any analyzed well. This rapid response started, and more importantly ended, much faster than the average turbidity responses in the N. Tafuna GUDI wells, where turbidity spikes tended to show an exponential decay back to the baseline turbidity value, a phase which usually lasted for days. In contrast, the quick return to baseline at Well 169, within a matter of hours, likely indicates that the casing leak stops once surface water flooding subsides. This example helps validate the premise that surface-water travel time in wells with compromised casings is short, on the order of hours as opposed to days, and further supports the conclusion that overly-permeable aquifer material causes the N. Tafuna GUDI issue.

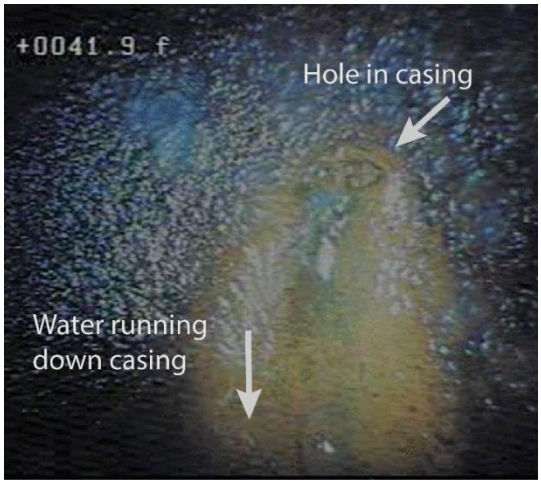

Figure 2.11: Horizontally oriented screen shot from borehole video log of Well 169 showing location of hole in casing and water actively cascading through the breach and down the well bore. Log was taken during a heavy rain event. Number in upper left corner indicates depth from surface in feet.

2.4.2 Isotope Mixing Model: Recent-Rainfall and Old-Groundwater Fractions

The high-resolution water-isotope well sampling in April 2016 took place during a period where $\delta^{18}O$ and $\delta^{2}H$ values in precipitation were substantially different from the reasonably consistent average annual isotopic composition of Tutuila's groundwater. This provided a short-term and seasonally dependent groundwater age dating tool, whereas recently recharged groundwater (i.e., recent-rainfall) and seasonally-integrated basal groundwater (i.e., old-groundwater) could be differentiated. By conceptualizing production well water as a mixture of these two isotopically-distinctive end-members, a basic isotope mixing model could be applied to quantify the fraction of water originating from each source. Isotope mixing models are commonly used for identifying the relative contribution of material in a mixed sample from different sources (e.g., Brooks et al. 2012; Fry 2013; Bishop et al. 2015). The isotope mass-balance approach is simple to apply for two end-member systems and results in a linear mixing relationship via integrating and solving a system of two equations of the form:

$$\delta_R \times F_R + \delta_{GW} \times F_{GW} = \delta_{MIX} \quad (2.)$$

$$F_R + F_{GW} = 1 \quad (3.)$$

Where

$\boldsymbol{\delta_R}$ is the isotopic composition of recent-rainfall collected during the precipitation event,
$\boldsymbol{\delta_{GW}}$ is the average annual isotopic composition (from monthly samples) of water at each well,
$\boldsymbol{\delta_{MIX}}$ is the isotopic composition of well samples, as a mix of recent rainfall and old-groundwater,
$\boldsymbol{F_R}$ is the calculated fraction of water originating from recent-rainfall,
$\boldsymbol{F_{GW}}$ is the calculated fraction of old-groundwater originating from the basal aquifer.

When applied to each $\delta^{18}O$ and $\delta^{2}H$ value measured during the rain-event sampling period, the mixing model provided end-member fractions at each well and at each point in time. Table 2.4 summarizes these fractions as percentages of recent-rainfall (specifically from the storm event sample) in each groundwater sample. The fraction of old-groundwater can be inferred as one minus this percentage. Table 2.4 includes dates where maximum and minimum fractions were calculated for each well, and temporal variability in these fractions can be visualized through direct comparison to isotopic values in Fig. 2.8.

Maximum fractions of recent-rainfall were observed in GUDI wells, 33 and 46, on the 15th and 17th of April, respectively, about a week after the start of the rain event, and also about when the period of rainy weather was transitioning to drier conditions. Although GUDI wells 81 and 72 were sampled at low resolution, the two data points collected from these wells show significant variation within the event-scale survey, with 53% to 47% of their water being sourced from recent-rainfall, respectively, during the heavy rain event portion of the

sampling period on April 11th. When these wells were sampled again during the drier portion of the sampling period, their isotope compositions had returned much of the way to the average annual groundwater isotope composition as sampled monthly throughout the year at Well 81. Unfortunately, it is unknown how the isotopic composition of waters at Wells 81 and 72 varied throughout the sample-period.

In general, results from the isotope-mixing model support the conclusions from the other tracers applied in this study. In wells 33, 46, 81 and 72, which are located close together within the Tafuna Lavas, up to one-third of the water produced was seen to be recently recharged rainfall. However, this fraction was no more than 3-4% in wells 84 and 93, which are located in the more ash rich Leone geologic unit. Well 89 showed an intermediate amount of variation during the sampling period, which may be due to its location at the northern margin of the Tafuna Lavas. The spatial distribution of variation seen in water isotopes, water levels, and in other tracers, suggests that an additional sub-division of the Tafuna geologic unit may be warranted. Wells within the N. Tafuna area all display a similar tracer response that is consistent with the GUDI determinations, whereas this response is reduced with distance from this area, and non-existent in the southern Tafuna wells.

Table 2.4: Results from isotope mixing model applied to a series of eight rain-event samples taken every other day between 4/10/2016 and 4/22/2016. Maximum and minimum calculated fractions of the recently recharged groundwater end-member are shown as percentages with the sample date of minimum or maximum occurrence shown in parentheses. Average annual groundwater end member values are specific to each well.

Well #	Average annual groundwater end member [δ^2H]	Maximum recent fraction and date of occurrence (in parentheses)	Minimum recent fraction and date of occurrence (in parentheses)
81 (GUDI)**	-20.49 ‰	53% (4/11)	22% (4/22)
72 (GUDI)**	-20.49 ‰*	47% (4/11)	21% (4/22)
33 (GUDI)	-20.45 ‰	38% (4/15)	14% (4/10)
46 (GUDI)	-20.45 ‰*	35% (4/17)	15% (4/10)
89 (GUDI)	-20.35 ‰	9% (4/17)	5% (4/10)
93 (non-GUDI)	-19.33 ‰	3% (4/23)	-6% (4/15)
84 (non-GUDI)	-19.18 ‰	4% (4/17)	-1% (4/10)

* Wells 46 and 72 were not measured monthly, end member values assumed from wells 81 and 33, respectively

** Wells 81 and 72 were only sampled twice, on 4/11 and 4/22

Note: Only δ^2H values and calculations shown, $\delta^{18}O$ calculations showed nearly equivalent fractions

2.5 Conclusions

Contaminated groundwater from GUDI wells in American Samoa has necessitated one of the longest standing boil-water notices in U.S. history. Effective management of this issue relies on understanding if causes are rooted in well construction problems or aquifer structure problems. This question was explored here through field measurements of three independent multi-tracer datasets including turbidity, indicator bacteria, and water isotopes. Observed tracer responses to rainfall were assessed through the premise that surface-water derived contamination from faulty well construction should arrive at well pumps more quickly than contamination resulting from rapid aquifer transit. Specifically, as exemplified by Well 169, travel times of 3 to 4 hours were observed where a casing breach was found, whereas expected transit time through Tafuna aquifer material was estimated at 21 to 30 hours. Observations from N. Tafuna wells revealed average tracer breakthrough times of 37 ± 21 hours for turbidity, 18 to 63 hours for bacteria, and 1 to 5 days for water isotopes. Travel times from all three methods are generally comparable, and all methods support the conclusion that overly-permeable aquifer material, as opposed to faulty well casings, is the most probable mechanism of contamination in the N. Tafuna GUDI wells.

Any one of the travel time estimates from the three methods used would probably be sufficient to determine which contamination mechanism is most likely. However, a coordinated assessment of all three tracers provided multiple opportunities for validation, gave deeper insight into the subtleties of aquifer conditions, and helped to explain the unique and sometimes enigmatic responses observed in some wells. Although Tutuila's wells have been categorized into a bimodal classification of GUDI or non-GUDI, in reality, each lies on a spectrum of influences controlled by heterogeneous and complex hydrogeology. The results of this study, at the very least can be used to confidently inform local water resource managers about the need for additional filtration infrastructure or abandonment of all wells in the N. Tafuna area. Repair or replacement will only result in continued GUDI contamination. However, observations of how tracer breakthroughs are shaped by heavy rainfall at each of the island's wells also provides insight into recharge dynamics, intra-aquifer variability, and subsurface flow characteristics of these and other highly-permeable young basaltic aquifers. The combination of physical, microbial, and isotopic tracers in this setting is a unique methodology that provides a valuable opportunity to better understand similarities and differences in how each tracer can be applied and interpreted to address water quantity and quality issues in geologically similar settings.

References: Chapter 2

ASCC - American Samoa Community College. 2018. Malaeimi weather station data. https://www.wunderground.com/personal-weather-station/dashboard?ID=IWESTERN499 (accessed 2018-04-30).

AS-DOC - Amercan Samoa Department of Commerce. 2013. The 2013 Statistical Yearbook for American Samoa. Pago Pago, AS: Amercan Samoa Department of Commerce. http://doc.as.gov/wp-content/uploads/2011/06/2013-Statistical-Yearbook-Final-Draft.pdf.

Barrell, R.A.E., and M.G.M. Rowland. 1979. The relationship between rainfall and well water pollution in a West African (Gambian) village. *Epidemiology & Infection* 83, no. 1: 143--150.

Birkel, C., J. Geris, M. Molina, C. Mendez, R. Arce, J. Dick, D. Tetzlaff, and C. Soulsby. 2016. Hydroclimatic controls on non-stationary stream water ages in humid tropical catchments. *Journal of hydrology* 542: 231--240.

Bishop, J.M., C.R. Glenn, D.W. Amato, and H. Dulai. 2017. Effect of land use and groundwater flow path on submarine groundwater discharge nutrient flux. *Journal of Hydrology: Regional Studies* 11: 194--218.

Brooks, J.R., P.J. Wigington, D.L. Phillips, R. Comeleo, and R. Coulombe. 2012. Willamette River Basin surface water isoscape ($\delta^{18}O$ and $\delta^{2}H$): temporal changes of source water within the river. *Ecosphere* 3, no. 5: 1--21.

Byappanahalli, M., and R. Fujioka. 1998. Evidence that tropical soil environment can support the growth of Escherichia coli. *Water Science and Technology* 38, no. 12: 171--174.

Byappanahalli, M.N., B.M. Roll, and R.S. Fujioka. 2012. Evidence for occurrence, persistence, and growth potential of Escherichia coli and enterococci in Hawaii's soil environments. Microbes and environments 27, no.2: 164--170.

Calderon, H., and S. Uhlenbrook. 2016. Characterizing the climatic water balance dynamics and different runoff components in a poorly gauged tropical forested catchment, Nicaragua. *Hydrological Sciences Journal* 61, no. 14: 2465--2480.

Cobb, K.M., J.F. Adkins, J.W. Partin, and B. Clark. 2007. Regional-scale climate influences on temporal variations of rainwater and cave dripwater oxygen isotopes in northern Borneo. *Earth and Planetary Science Letters* 263, no. 3-4: 207--220.

Dansgaard, W. 1964. Stable isotopes in precipitation. *Tellus* 16, no.4: 436--468.

Entry, J.A., and N. Farmer. 2001. Movement of coliform bacteria and nutrients in ground water flowing through basalt and sand aquifers. *Journal of Environmental Quality* 30, no. 5: 1533--1539.

Fackrell, J.K. 2016. Geochemical evolution of Hawaiian groundwater. Honolulu, HI: Doctoral dissertation, University of Hawai'i at Manoa. https://www.soest.hawaii.edu/GG/resources/theses/JFackrell_Dissertation.pdf.

FAO - Food and Agriculture Organization of the United Nations. 2016. AQUASTAT website. http://www.fao.org/nr/water/aquastat/water_use/ (accessed 2018-03-07).

Foppen, J., and J. Schijven. 2006. Evaluation of data from the literature on the transport and survival of Escherichia coli and thermotolerant coliforms in aquifers under saturated conditions. *Water Research* 40, no. 3: 401--426.

Freeze, R.A., and J.A. Cherry. Groundwater. (Englewood Cliffs, New Jersey: Prentice Hall, 1979).

Fry, B. 2013. Alternative approaches for solving underdetermined isotope mixing problems. *Marine ecology progress series* 472: 1--13.

Gat, J.R. 1996. Oxygen and hydrogen isotopes in the hydrologic cycle. *Annual Review of Earth and Planetary Sciences* 24: 225--262.

Glickman, T.S. 2000. Glossary of Meteorology. American Meteorological Society, 2nd Edn. MA, USA: American Meteorological Society. http://glossary.ametsoc.org/wiki/Rain.

Godfrey, S., F. Timo, and M. Smith. 2005. Relationship between rainfall and microbiological contamination of shallow groundwater in Northern Mozambique. *Water Sa* 31, no.4: 609--614.

Goldscheider, N., M. Pronk, and J. Zopfi. 2010. New insights into the transport of sediments and microorganisms in karst groundwater by continuous monitoring of particle-size distribution. *Geologia Croatica* 63, no. 2: 137--142.

Izuka, S.K., J.A. Perreault, and T.K. Presley. 2007. Areas contributing recharge to wells in the Tafuna-Leone Plain, Tutuila, American Samoa. Honolulu, HI: Geological Survey (US). Report no. 2007-5167. https://pubs.er.usgs.gov/publication/sir20075167.

Keating, B.H., and B.R. Bolton. Geology and offshore mineral resources of the Central Pacific Basin. (New York, NY: Springer Science \& Business Media, 1992).

Kiernan, K., C. Wood, and G. Middleton. 2003. Aquifer structure and contamination risk in lava flows: insights from Iceland and Australia. *Environmental Geology* 43, no. 7: 852--865.

Kirs, M., P. Moravcik, P. Gyawali, K. Hamilton, V. Kisand, I. Gurr, C. Shuler, and W. Ahmed. 2017. Rainwater harvesting in American Samoa: current practices and indicative health risks. *Environmental Science and Pollution Research* 24, no. 13: 12384--12392.

Kresic, N. Hydrogeology and groundwater modeling. (Boca Raton, Fl: CRC press, 2006).

Levitt, D.G., D.L. Newell, W.J. Stone, and D.S. Wykoff. 2005. Surface Water--Groundwater Connection at the Los Alamos Canyon Weir Site. *Vadose Zone Journal* 4, no. 3: 708--717.

Massei, N., J. Dupont, B. Mahler, B. Laignel, M. Fournier, D. Valdes, and S. Ogier. 2006. Investigating transport properties and turbidity dynamics of a karst aquifer using correlation, spectral, and wavelet analyses. *Journal of hydrology* 329, no. 1-2: 244--257.

Mauga, D. 2016. Personal Communication

Nakamura, S., 1984, Soil Survey of American Samoa: U.S. Department of Agriculture Soil Conservation Service, 95 p.

Pronk, M., N. Goldscheider, J. Zopfi, and F. Zwahlen. 2009. Percolation and particle transport in the unsaturated zone of a karst aquifer. *Groundwater* 47, no. 3: 361--369.

Rhodes, A.L., A.J. Guswa, and S.E. Newell. 2006. Seasonal variation in the stable isotopic composition of precipitation in the tropical montane forests of Monteverde, Costa Rica. *Water Resources Research* 42, no. 11.

Rozanski, K., L. Araguas-Araguas, R. Gonfiantini. 1993. Isotopic patterns in modern global precipitation. In: Swart, P.K., K.C. Lohmann, J. McKenzie (Eds.), Climate Change in Continental Isotopic Records. *Geophysical Monograph* 78: 1--36

Scholl, M.A., S.B. Gingerich, and G.W. Tribble. 2002. The influence of microclimates and fog on stable isotope signatures used in interpretation of regional hydrology: East Maui, Hawaii. *Journal of Hydrology* 264, no. 1-4: 170--184.

Scholl, M.A., S.E. Ingebritsen, C.J. Janik, and J.P. Kauahikaua. 1996. Use of precipitation and groundwater isotopes to interpret regional hydrology on a tropical volcanic island: Kilauea volcano area, Hawaii. *Water Resources Research* 32, no. 12: 3525--3537.

Stearns, H.T. 1944. Geology of the Samoan islands. *Bulletin of the Geological Society of America* 55, no. 11: 1279--1332.

Taylor, R., A. Cronin, S. Pedley, J. Barker, and T. Atkinson. 2004. The implications of groundwater velocity variations on microbial transport and wellhead protection--review of field evidence. *FEMS Microbiology Ecology* 49, no. 1: 17--26.

US-EPA - U.S. Environmental Protection Agency. 1998. National Primary Drinking Water Regulations: Enhanced Surface Water Treatment Rule. Washington, DC.: U.S. Environmental Protection Agency. https://www.epa.gov/dwreginfo/surface-water-treatment-rules.

US-EPA - U.S. Environmental Protection Agency. 2006. National Primary Drinking Water Regulations: Ground Water Rule. Washington, DC.: U.S. Environmental Protection Agency. https://www.epa.gov/dwreginfo/ground-water-rule.

Vold, S., J. Regis, and J. Gambatese. 2013. Groundwater Under the Direct Influence of Surface Water Study: Well 81. unpublished report submitted to American Samoa Environmental Protection Agency. Pago Pago, AS: Amercan Samoa Power Authority.